Electrochemical Behavior of Ferredoxins Adsorbed on Mercury Electrode Surface. Cyclic d.c. and a.c. Voltammetric Studies with Hanging Mercury Drop Electrode

Tokuji IKEDA,* Kazunobu TORIYAMA, and Mitsugi SENDA

Department of Agricultural Chemistry, Kyoto University, Sakyo-ku, Kyoto 606

(Received December 25, 1978)

The electrochemical behavior of *Clostridium pasteurianum* ferredoxin and spinach ferredoxin was studied by cyclic d.c. and cyclic phase-selective a.c. voltammetry with a hanging mercury drop electrode. An irreversible adsorption of these ferredoxins on the electrode surface is described. In successive cyclic voltage scans both d.c. and a.c. voltammograms of ferredoxins change gradually in both height and form until a steady state is attained, indicating that the ferredoxins adsorbed on the electrode surface decompose to cluster-free ferredoxins. Apoferredoxins give the same voltammograms as the steady state voltammograms of ferredoxins. The steady state voltammograms are assigned to RSH/RSHg redox reaction of the cysteine residues in apoferredoxin. At pH lower than 8 the d.c. waves are explained by an equation for reversible one-electron surface redox reaction. Kinetic parameters of the redox reaction were determined by a.c. voltammetry.

Ferredoxins, iron-sulfur proteins, function as electron carriers in many metabolic reactions.[1] The standard oxidation-reduction potential, E_0', and the stoichiometry of electron equivalents, n', of various ferredoxins have been measured by equilibrium techniques.[2] Attempts to measure the E_0' value directly by polarography have also been made.[3-8] Although the technique may be an advantageous means of studying the oxidation-reduction reaction of ferredoxins, the exact relationship between half-wave potential and E_0' requires further examination. In this study the electrochemical reduction and oxidation of two types of ferredoxins were examined with use of cyclic d.c. and a.c. voltammetry to gain a better understanding of their electrochemical behavior. Here we use the term "cyclic d.c. voltammetry" in place of the ordinary cyclic voltammetry in order to distinguish this technique from "cyclic a.c. voltammetry,"[9] in which alternating voltage of small amplitude is superimposed upon the cyclic sweep voltage applied to the electrode and the alternating currents (both in-phase and out-of-phase components, using a phase-selective amplifier) are measured as a function of the cyclic sweep voltage in both cathodic and anodic sweeps.

Part A. Cyclic d.c. Voltammetry

Experimental

Materials. Clostridium Pasteurianum Ferredoxin (Cl.Fd) and Spinach Ferredoxin (sp.Fd): Ferredoxins from *Clostridium pasteurianum* (ATCC 6013) and spinach were prepared according to the method of Mayhew,[10] the Cl.Fd having an absorption ratio of 0.78 or greater (390/280 nm) and sp.Fd one of 0.45 or greater (420/275 nm). The ferredoxin concentrations of stock solutions were determined spectrophotometrically with molar extinction coefficients of 3.0×10^4 at 390 nm[10] and 9.7×10^3 at 420 nm[11] for Cl.Fd and sp.Fd, respectively. The stock solutions were stored at 4 °C anaerobically.

Apoferredoxin from Clostridium Pasteurianum (apo-Cl.Fd): Iron and acid-labile sulfide were removed from Cl.Fd by treatment of the protein with an acid. Thirty microliters of *ca.* 0.5 mM Cl.Fd was acidified with 30 μl of 0.4 M hydrogen chloride. Hydrogen sulfide evolved was expelled by passing nitrogen gas through the solution. The brown color of ferredoxin disappeared completely after *ca.* 10 min, a white precipitate being formed. The solution was neutralized with 0.4 M sodium hydroxide to dissolve the precipitate and 3 μl of 0.05 M disodium ethylenediaminetetraacetate was added to the solution.

All other chemicals used were highly pure commercial products (Nakarai Chemicals Co., Ltd.). Triply distilled water was used to prepare the electrolysis solution.

Instruments. Cyclic d.c. voltammograms were recorded on a Yanagimoto PE21-TB2S potentiostat with a built-in sweep voltage generator and a Yokogawa X-Y recorder. A Metrohm E410 hanging mercury drop electrode was used, the surface area of the electrode being 0.0187 ± 0.0003 cm^2.

Electrochemical Measurements. All measurements were made with a three-electrode potentiostat. Potentials were measured against a saturated calomel electrode (SCE). Buffer solutions (0.1 M hydrogen chloride–sodium acetate for pH 1.4—4.0, 0.1 M acetic acid–sodium acetate for pH 4.0—5.5, 0.1 M sodium dihydrogenphosphate–disodium hydrogenphosphate for pH 5.5—7.0, 0.1 M hydrogen chloride–tris(hydroxymethyl)aminomethane for pH 7.0—9.2 and 0.1 M glycine–sodium hydroxide for pH 9.2—11.0) were used as the base solution. The ionic strength of the base solution was adjusted to 0.5 mol/kg with sodium chloride. To avoid possible complications associated with the foaming of the solution, 3 ml of the base solution was transferred to the cell and deaerated for *ca.* 10 min by passing nitrogen gas, which had previously been passed through a solution of the same composition as that of the base solution. An aliquot of the stock solution of ferredoxin was then introduced into the base solution with a microsyringe under nitrogen atmosphere. A fresh mercury drop from the hanging mercury drop electrode (HMDE) was exposed to the solution for a given period of time (t_{exp}), while the potential of the HMDE was kept controlled at a constant potential (E_i). The voltage scan was then started from E_i, with a scan rate $v=0.36$ V s^{-1}, unless otherwise stated. All experiments were carried out at 25 °C.

Results

Cl.Fd. Figure 1 shows a typical single sweep voltammogram of 1.2 μM Cl.Fd in pH 6.6 phosphate buffer, which was recorded after $t_{exp}=2$ min at $E_i=-0.1$ V. In addition to a catalytic wave (a presodium wave) at -1.7 V, a peak-shaped wave appeared at -0.57 V. It grew up to a certain limit with increasing concentration of Cl.Fd at a constant exposure time or with increasing exposure time at a constant

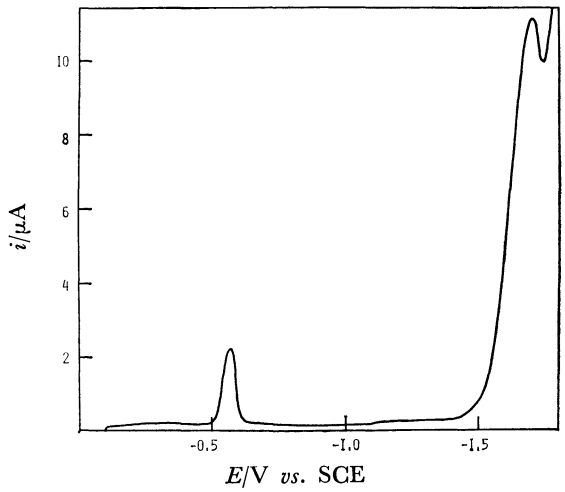

Fig. 1. d.c. voltammogram of 1.2 μM Cl.Fd in pH 6.6 phosphate buffer. Voltage scan was started from $E_i = -0.1$ V after $t_{exp} = 2$ min.

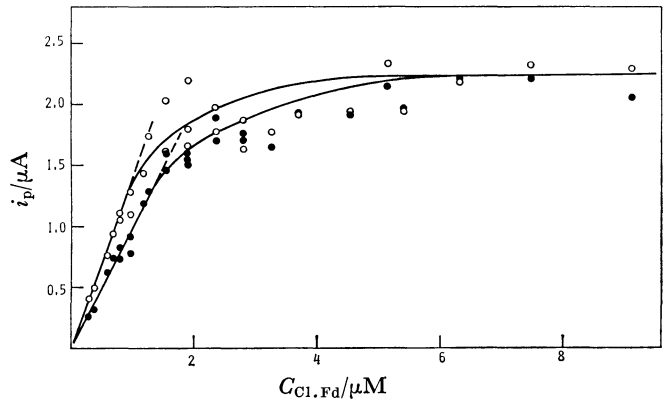

Fig. 2. The plot of i_p against $C_{Cl.Fd}$ at pH 6.9. ●: $t_{exp} = 17.5$ s, ○: $t_{exp} = 32.5$ s.

concentration of Cl.Fd, indicating that the wave is due to the Cl.Fd accumulated on the electrode surface. The dependence of peak height, i_p, of the wave on the Cl.Fd concentration, $C_{Cl.Fd}$, is shown in Fig. 2 for two t_{exp} values at pH 6.9. At lower concentrations of Cl.Fd the dependence of i_p on $C_{Cl.Fd}$ is linear, the product $C_{Cl.Fd} \times t_{exp}^{1/2}$ remaining constant for a given i_p value. This is evidence of the diffusion-controlled adsorption of Cl.Fd at the electrode surface, the current being assumed to be proportional to the surface concentration of Cl.Fd.[12-14]

Figure 3 shows cyclic voltammograms for Cl.Fd adsorbed on the HMDE at pH 9.2; the voltammograms were recorded after $t_{exp} = 1$ min at $E_i = -0.1$ V(Fig. 3A) and at -1.1 V (Fig. 3B). When the voltage scan was started from $E_i = -0.1$ V, two cathodic waves (Fig. 3A, I and II) were observed at -0.67 V and -0.78 V, respectively. Upon reversal of the scan at -1.1 V, two anodic waves(Fig. 3A, III and IV) appeared at -0.78 V and -0.63 V, respectively. In the second cycle of the voltage scan between -0.1 V and -1.1 V, the wave IV almost disappeared. In the successive voltage scans wave I decreased in height and finally disappeared, whereas the heights of waves II and III increased slightly until a steady

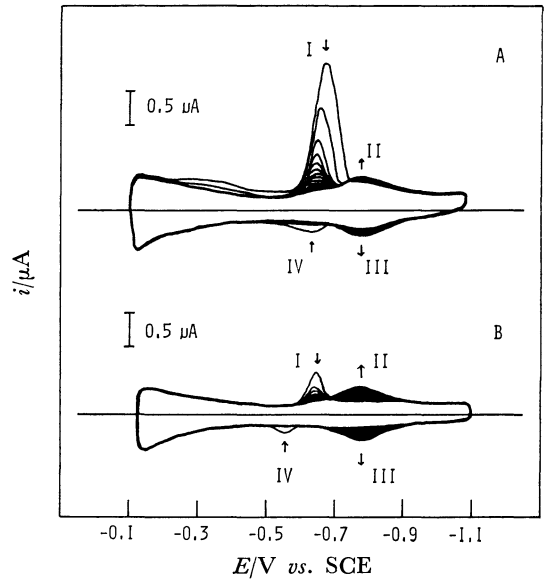

Fig. 3. Cyclic d.c. voltammograms of 1.9 μM Cl.Fd in pH 9.2 glycine buffer. Voltage scan was started from (A) $E_i = -0.1$ V and (B) $E_i = -1.1$ V after $t_{exp} =$ 1 min.

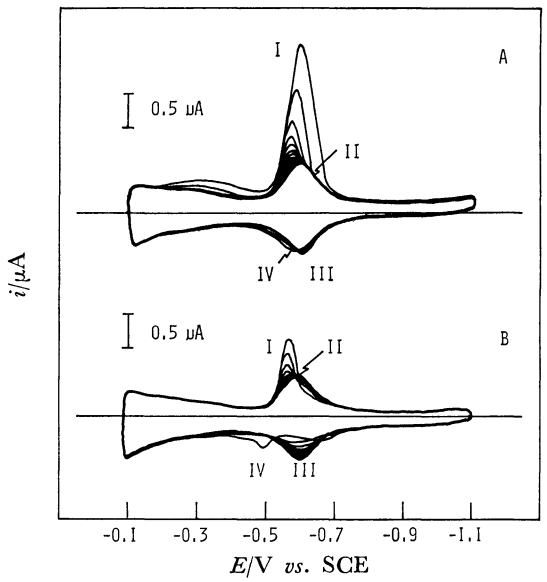

Fig. 4. Cyclic d.c. voltammograms of 1.9 μM Cl.Fd in pH 6.9 phosphate buffer. Voltage scan was started from (A) $E_i = -0.1$ V, (B) $E_i = -1.1$ V after $t_{exp} =$ 1 min.

state was attained. When the voltage scan was started from $E_i = -1.1$ V after $t_{exp} = 1$ min (Fig. 3B), a small anodic wave IV was observed and a cathodic wave I in the reverse cathodic scan. However, wave IV disappeared in the second cyclic scan. In successive voltage scans, the height of wave I decreased and waves III (anodic) and II (cathodic) of nearly equal wave height appeared at -0.78 V, their heights increasing until a steady state was attained. The shape and height of the waves II and III at the steady state are independent of E_i.

Figure 4 shows cyclic voltammograms for Cl.Fd adsorbed on the HMDE surface at pH 6.9 after $t_{exp} =$

Table 1. Scan rate dependence of peak current, peak potential and half-peak width of wave II (cathodic) and wave III (anodic) at the steady state

Ferredoxin	v / V s^{-1}	$10^2\, i_p^{DC}$/μA		E_p^{DC}/V		$\Delta E_{p/2}^{DC}$/mV	
		II	III	II	III	II	III
Cl.Fd (at pH 6.9)	0.09	12	13	−0.60	−0.60	90	90
	0.18	25	25	−0.60	−0.60	85	90
	0.27	35	33	−0.60	−0.60	90	95
	0.36	45	47	−0.60	−0.60	90	95
sp.Fd (at pH 6.6)	0.09	3.2	2.9	−0.59	−0.58	95	100
	0.18	6.8	6.0	−0.59	−0.58	95	100
	0.36	14	12	−0.59	−0.58	95	105

1 min at $E_i = -0.1$ V (Fig. 4A) and at -1.1 V (Fig. 4B). The two cathodic waves (I and II) and the two anodic waves (III and IV), though not well separated, changed in height in successive voltage scans in nearly the same way as at pH 9.2, waves II (cathodic) and III (anodic) with identical peak potential of -0.60 V appearing on the cyclic voltammogram in the steady state.

The behavior of successive cyclic voltammograms of Cl.Fd at pH 9.2 and 6.9 indicates that the Cl.Fd adsorbed on the HMDE surface decomposes irreversibly and that waves II and III are due to the redox reaction of the decomposition product. The scan rate dependence of the peak currents, i_p(II) and i_p(III), the peak potentials, E_p^{DC}(II) and E_p^{DC}(III), and the half-peak widths, $\Delta E_{p/2}^{DC}$(II) and $\Delta E_{p/2}^{DC}$(III), of waves II and III at the steady state at pH 6.9 are summarized in Table 1. Both i_p(II) and i_p(III) are proportional to v, the ratio i_p(II)/i_p(III) being unity. E_p^{DC}(II) and E_p^{DC}(III) coincide with each other and are independent of v. The half-peak widths of these waves are 91±2 mV over the scan-rate range 0.09 V s^{-1}—0.36 Vs^{-1}. The results indicate that the reaction corresponding to waves II and III at pH 6.9 is a reversible one-electron surface redox reaction.[15] The pH dependence of E_p^{DC}(II) ($=E_p^{DC}$(III)) is shown in Fig. 5. E_p^{DC} shifts by -60 mV/pH at pH lower than 8 but more at pH higher than 8. The integrated current at pH 6.9 was calculated to be Q(II)=9.5± 1.0 μC cm^{-2} for wave II and Q(III)=8.0±0.5 μC cm^{-2} for wave III.

Apo-Cl.Fd. Cyclic voltammetry was performed with apo-Cl.Fd solution under experimental conditions similar to those for the native Cl.Fd. When the voltage scan was started from $E_i = -1.0$ V after t_{exp}=1 min, only waves II and III (Fig. 6A) appeared on the cyclic voltammogram of the first cyclic scan, remaining unchanged on the successive scans. One more cathodic wave, that is wave I in Fig. 6B, was observed when the voltage scan was started from $E_i = -0.1$ V after t_{exp}=1 min. However the wave almost disappeared in the second cathodic scan. The behavior of waves II and III for apo-Cl.Fd was the same as that of waves II and III for Cl.Fd in the steady state.

Sp.Fd. The same series of experiments were performed with sp.Fd. The cyclic voltammogram for sp.Fd in the steady state is shown in Fig. 7. The scan rate dependence of the peak current, peak potential and half-peak width is summarized in Table 1. The integrated current of the waves was calculated to be Q =3.2±0.4 μC cm^{-2}.

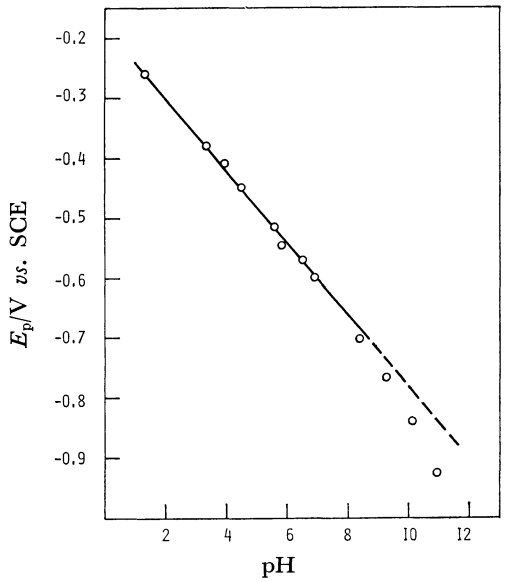

Fig. 5. Dependence of the peak potential, E_p^{DC}(II) ($=E_p^{DC}$(III)) on pH of the steady-state waves II and III.

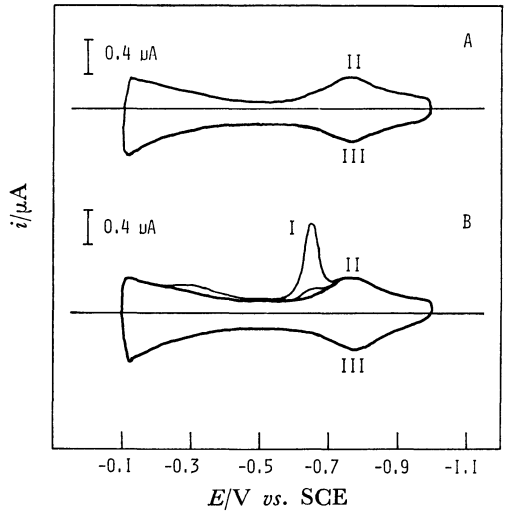

Fig. 6. Cyclic d.c. voltammograms for apo-Cl.Fd at pH 9.2. Voltage scan was started from (A) $E_i = -1.0$ V and (B) $E_i = -0.1$ V after t_{exp}=1 min.

Discussion

Adsorption of Ferredoxin on the Electrode Surface. Experimental results give evidence of an irreversible adsorption of ferredoxins on the surface of a mercury electrode. This was confirmed by the following experiment. After Cl.Fd had accumulated at the electrode surface, the electrode was removed from the protein-containing solution and washed with distilled water. The electrode was then placed in the base

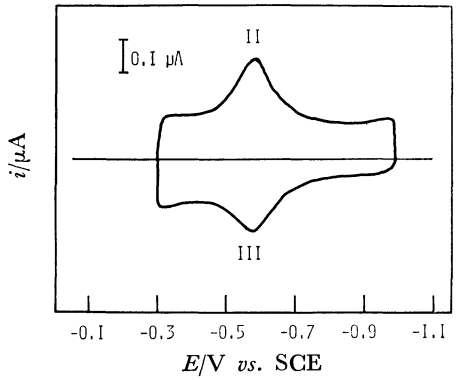

Fig. 7. Cyclic d.c. voltammogram at the steady state for sp.Fd at pH 6.6.

solution and voltammograms were recorded which were found to be the same as those in the case of an ordinary experiment with a solution containing Cl.Fd. Several workers[3,6,16] have suggested the adsorption of ferredoxins on a mercury electrode surface. Experimental results also indicate that the adsorption of ferredoxin is controlled by diffusion; at low concentrations of Cl.Fd $i_p=kq\Gamma=kq2(D_{Cl.Fd}/\pi)^{1/2}\ t_{exp}^{1/2}C_{Cl.Fd}$, where k is the proportionality constant, q the surface area of HMDE, Γ the surface concentration of Cl.Fd and $D_{Cl.Fd}$ the diffusion coefficient of Cl.Fd. At high concentrations a maximum current is attained, which can be given by $i_p^{max}=kq\Gamma^{max}$, where Γ^{max} is the maximum surface concentration of adsorbed Cl.Fd. Combining these two equations, we estimated the Γ^{max} value as 1.28×10^{-11} mol cm^{-2}, $D_{Cl.Fd}$ being calculated to be 1.4×10^{-6} cm^2 s^{-1} from the Svedberg equation with $s_{20,w}=1.4$ s, $v=0.63$ cm^3 g^{-1} [17] and $M.W.=6200$.[18] The value of Γ^{max} is in the order of magnitude comparable to that of other proteins.[19]

Waves I and IV. The value of integrated current of wave I was 19—30 μC cm^{-2} which is too large for this wave to be ascribed to the reduction of the biologically active cluster of Cl.Fd adsorbed on the electrode surface. A possible explanation is that the wave is due to the hydrogen evolution reaction catalyzed by the cluster of adsorbed Cl.Fd molecule, which decomposes in successive voltage scans. The large cathodic wave observed with apo-Cl.Fd in the first negative-going scan should be attributed to the residual amount of the active cluster.

The anodic wave IV may correspond to the oxidation of the cluster since it was not observed with apo-Cl.Fd. The corresponding cathodic wave may be concealed by the large cathodic hydrogen evolution current. It is difficult to study the redox reaction of the cluster by the present method.

Waves II and III. Waves II and III attain a steady state in successive voltage scans. Apo-Cl.Fd also gives the same waves as II and III of Cl.Fd in the steady state. The results indicate that waves II and III are due to the redox reaction of apoferredoxin produced by decomposition of the ferredoxin adsorbed on the electrode surface. Kuznetsov *et al.*[16] have also suggested the decomposition of the cluster of ferredoxin and the release of sulfhydryl groups on the electrode surface. The behavior of these waves (Table 1) can be explained by the equation for reversible one-electron surface redox reaction[15]

$$i = (n^2F^2/RT)qvn_c\Gamma^{max}\exp(\varphi)(1+\exp(\varphi))^{-2}, \quad (1)$$

where n is the number of electrons of the redox couple ($n=1$ in the present case), n_c the number of redox couples in one molecule of adsorbed ferredoxin and $\varphi=(nF/RT)(E-E_p^{pc})$. The results together with the pH-dependence of the peak potential indicate that the reversible one-electron wave may be assigned to RSH+Hg=RSHg+H$^+$+e$^-$. By substituting i_p values of Cl.Fd (Table 1) and $\Gamma^{max}=1.28\times10^{-11}$ mol cm^{-2} into Eq. 1 at $E=E_p^{pc}$, n_c was estimated to be 7.3±0.6. n_c was estimated to be 7.3±1.0 from the equation $Q=n_cF\Gamma^{max}$ with $Q=(1/2)(9.5+8.0)=8.7\pm1.0$ μC cm^{-2} and $\Gamma^{max}=1.28\times10^{-11}$ mol cm^{-2}. These n_c value are approximately 8, the number of cysteine residues of apo-Cl.Fd molecule. In the case of sp.Fd, n_c was estimated to be 5.2 with $Q=3.2$ μC cm^{-2} and $\Gamma^{max}=(1/2)1.28\times10^{-11}$ mol cm^{-2}, which is 5, the number of cysteine residues of apo-sp.Fd molecule. The redox mechanism corresponding to waves II and III can be assigned to (Apo-Fd(SH)$_{n_c}$)$_{ad}$+n_cHg⇌(Apo-Fd(SHg)$_{n_c}$)$_{ad}$+n_cH$^+$+n_ce$^-$, where $n_c=8$ for apo-Cl.Fd and 5 for apo-sp.Fd, at pH lower than 8.

At pH higher than 8 waves II and III become drawn out. Their wave heights decrease, the pH-dependence of the peak potential deviating from −60 mV/pH line. This indicates an involved nature of the surface redox reaction in basic solution Brown and Anson[20] have explained similar nonideal behavior of the cyclic voltammograms for reactions irreversibly attached to the surface of graphite electrode by introducing a nonideality parameter r; the surface activities used in place of the surface concentration are dependent on this parameter Another possible explanation is that the RSH/RSHg couples in apoferredoxin molecule may have different oxidation-reduction potentials which are distributed around the peak potential of the waves. Shift of the oxidation-reduction potentials associated with possible conformational changes of apoferredoxin adsorbed on the electrode surface should be taken into account.

Part B. Cyclic a.c. Voltammetry

Experimental

Experiments were performed with a Yanagimoto PE21-TB2S potentiostat with a built-in sweep voltage generator, an NF model LI572-B lock-in amplifier and a Yokogawa 3077 X-Y recorder. The amplitude of superimposed alternating voltage was adjusted to 10 mV (peak to peak) throughout the frequency range 100—700 Hz. Both resistive (in-phase) and capacitive (out-of-phase) components of the alternating currents (a.c.) were recorded against cyclic (d.c.) sweep voltage (usually $v=0.1$ V s^{-1}) applied to the HMDE For further details of the electrochemical measurements, *cf.* reference in part A.

Results

Figure 8 shows a typical cyclic in-phase a.c. voltammogram for Cl.Fd adsorbed on the HMDE surface

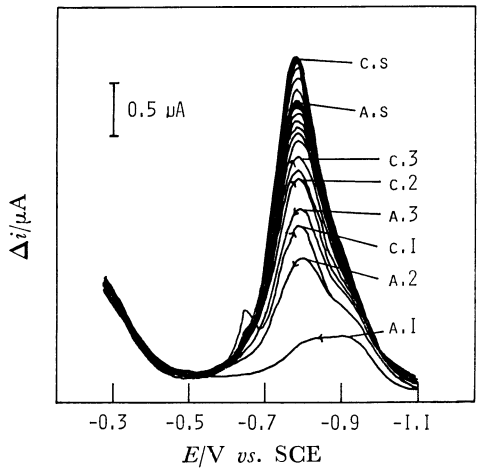

Fig. 8. Cyclic in-phase a.c. voltammogram of 1.9 μM Cl.Fd in pH 9.2 glycine buffer at $f=500$ Hz. d.c. voltage scan was started from $E_i=-1.1$ V after $t_{exp}=1$ min. A1,A2,A3: Voltammograms of first, second and third anodic scan, C1,C2,C3: voltammograms of first, second and third cathodic scan and AS and CS: steady state voltammograms of positive-going (anodic) and negative-going (cathodic) scan, respectively.

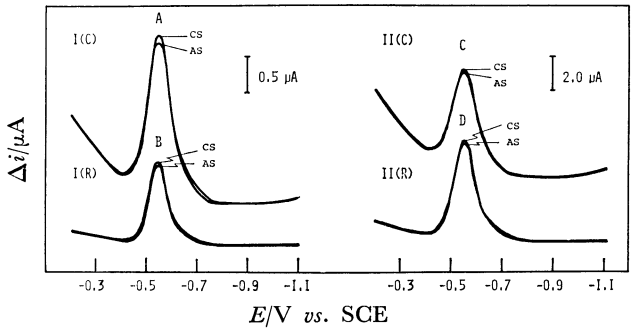

Fig. 9. Cyclic a.c. voltammograms at the steady state for Cl.Fd at pH 5.9. I(C) and I(R): Out-of-phase and in-phase component at $f=100$ Hz, II(C) and II(R): out-of-phase and in-phase component at $f=500$ Hz. AS and CS show voltammograms of positive-going and negative-going scan, respectively.

at pH 9.2. A saturation coverage of the electrode surface with Cl.Fd was attained by exposing the electrode to the solution for one minute at $E_i=-1.1$ V, the voltammogram then being recorded. In the first positive-going scan a small a.c. wave appeared in the potential region −0.70 V——1.0 V. Upon reversal of the scan at −0.27 V, two a.c. waves were observed at −0.65 V and −0.78 V. The wave at −0.65 V disappeared in successive voltage scans between −0.27 V and −1.1 V, whereas the wave at −0.78 V attained a steady state in the same successive scans. Apo-Cl.Fd gave essentially the same voltammogram as that of Cl.Fd in the steady state. The results indicate that the a.c. waves of Cl.Fd in the steady state are due to the redox reaction of apo-Cl.Fd adsorbed on the electrode surface.

Figure 9 shows the cyclic a.c. voltammograms in the steady state for the adsorbed Cl.Fd at pH 5.9 at two a.c. frequencies. The peak potentials, E_p^{AC}, of the four a.c. waves (A, B, C, and D) are independent

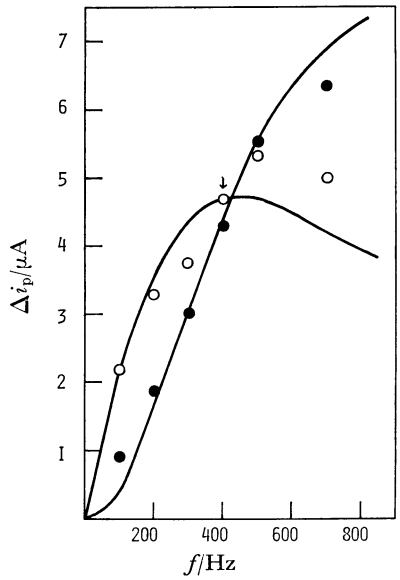

Fig. 10. Dependence of the a.c. peak currents on the a.c. frequency at pH 5.9. ○: Out-of-phase component and ●: in-phase component.

of a.c. frequency, coinciding with each other and with the peak potential of waves II and III of d.c. cyclic voltammogram at the same pH (Fig. 5). On the other hand, the peak height, Δi_p, and half-peak width, $\Delta E_{p/2}^{AC}$, of both in-phase and out-of-phase components are dependent on a.c. frequency (Fig. 10 and Table 2).

In basic solution of pH higher than 8, the a.c. voltammograms become drawn-out and decrease in height.

Discussion

According to theory of cyclic a.c. voltammetry[21] of a redox couple, ox/red, tightly adsorbed on the electrode surface, the capacitive (out-of-phase) and resistive (in-phase) components of the amplitude of a.c. currents, $\Delta i(C)$ and $\Delta i(R)$, are given by

$$\left.\begin{aligned}\Delta i(C) &= \frac{mnF^2qn_c\Gamma_t 2\pi f\Delta E}{RT}\times\frac{\exp(\varphi)}{(1+\exp(\varphi))^2}\times\frac{1}{((2\pi f/(\vec{k}+\overleftarrow{k}))^2+1)}\\ \Delta i(R) &= \frac{mnF^2qn_c\Gamma_t 2\pi f\Delta E}{RT}\times\frac{\exp(\varphi)}{(1+\exp(\varphi))^2}\times\frac{2\pi f/(\vec{k}+\overleftarrow{k})}{((2\pi f/(\vec{k}+\overleftarrow{k}))^2+1)}\end{aligned}\right\}\quad(2)$$

Here it is assumed that the redox reaction is expressed by a simple Butler-type equation $i/nFq=\overleftarrow{k}n_c\Gamma_{red}-\vec{k}n_c\Gamma_{ox}$ with $\overleftarrow{k}=k_s\exp((1-\alpha)\varphi)$, $\vec{k}=k_s\exp(-\alpha\varphi)$ and $\varphi=(nF/RT)(E^{DC}-E_0)$ and that the redox reaction is d.c.-voltammetrically reversible; $k_s/(nFv/4RT)\gg 1$. Γ_j is the surface concentration of j (j=ox and red, and $\Gamma_t=\Gamma_{ox}+\Gamma_{red}$), k_s the standard rate constant, α the transfer coefficient, m the proportionality constant,[21] in which the change of electrode charge associated with the change of Γ_j as well as n is involved, ΔE and f are the amplitude and frequency of superimposed alternating

TABLE 2. PEAK POTENTIAL AND HALF-PEAK WIDTH OF a.c. WAVES AT THE STEADY STATE FOR Cl.Fd ADSORBED ON MERCURY ELECTRODE SURFACE AT pH 5.9

f/Hz	E_p^{AC}/V	$\Delta E_{p/2}^{AC}$(R)[a]/mV		$\Delta E_{p/2}^{AC}$(C)[b]/mV	
		obsd	calcd	obsd	calcd
100	−0.55	80	74	95	92
200	−0.55	80	76	100	98
300	−0.55	85	80	110	106
400	−0.55	90	85	115	116
500	−0.55	95	90	120	126
700	−0.55	100	99	130	145

a) In-phase. b) Out-of-phase.

TABLE 3. STANDARD ELECTRON TRANSFER RATE CONSTANT OF FERREDOXINS ADSORBED ON MERCURY ELECTRODE SURFACE

pH	k_s[a]/10^2 s^{-1}
4.4	12.0±5.0[b]
5.9	13.4±3.7[b]
6.9	15.2±1.7[b]
6.9	10.1±3.1[c]
6.6	13.6±3.2[d]

a) Average value over the a.c. frequencies between 100 Hz and 700 Hz. b) Cl.Fd at the steady state. c) Apo-Cl.Fd. d) sp.Fd at the steady state.

voltage, respectively. At $E=E_0$, the ratio $\Delta i(\mathrm{R})/\Delta i(\mathrm{C})$ is given by

$$(\Delta i(\mathrm{R}))_{E=E_0}/(\Delta i(\mathrm{C}))_{E=E_0} = 2\pi f/2k_s \quad (3)$$

so that the k_s value can be determined experimentally provided that E_0 is known. As decribed above E_p^{AC} is independent of f and coincides with E_p^{DC} of corresponding *reversible* d.c. voltammograms, indicating that $E_p^{AC}=E_p^{DC}=E_0$ and α is at least not much different from 0.5. Application of Eq. 3 to experimental data, such as those shown in Fig. 10 gives k_s values summarized in Table 3. Solid lines in Fig. 10 are drawn by Eq. 2 at $E=E_0$ using $k_s=13.4\times10^2$ s^{-1} and $\Delta i_p(\mathrm{C})=4.7$ μA at 400 Hz. Values of $\Delta E_{p/2}^{AC}$ as calculated from Eq. 2 by assuming $n=1$ and $\alpha=0.5$ are also given in Table 2. Apparent agreement between theory and experiment is good in spite of the very simplified model of charge transfer kinetics. Kinetic study gives information on the protonation mechanism associated with the charge transfer, RSH+Hg=RSHg+H$^+$+e$^-$. When a very rapid (*i.e.* reversible) proton transfer to oxidized form is followed by the charge transfer as

$$\begin{aligned} &\mathrm{RSHg} + \mathrm{H^+} = (\mathrm{RSHg})\mathrm{H^+}, && K_\mathrm{I} \\ &(\mathrm{RSHg})\mathrm{H^+} + \mathrm{e^-} = \mathrm{RSH} + \mathrm{Hg}, && k_{s0\mathrm{I}} \end{aligned} \quad (\mathrm{I})$$

the "measured" or apparent standard rate constant k_s is given by

$$k_s = k_{s0\mathrm{I}}(1+K_\mathrm{I}/(\mathrm{H^+}))^{-(1-\alpha)} \quad (4)$$

where $k_{s0\mathrm{I}}$ is the standard rate constant and K_I the dissociation constant of (I). When the charge transfer is followed by a very rapid proton transfer to reduced form as

$$\begin{aligned} &\mathrm{RSHg} + \mathrm{e^-} = \mathrm{RS^-} + \mathrm{Hg}, && k_{s0\mathrm{II}} \\ &\mathrm{RS^-} + \mathrm{H^+} = \mathrm{RSH}, && K_\mathrm{II} \end{aligned} \quad (\mathrm{II})$$

the apparent standard rate constant k_s is given by

$$k_s = k_{s0\mathrm{II}}(1+(\mathrm{H^+})/K_\mathrm{II})^{-\alpha} \quad (5)$$

where $k_{s0\mathrm{II}}$ is the standard rate constant and K_II the dissociation constant of (II). k_s tends to increase with increasing pH (see Table 3). This supports mechanism (II). However, the change of k_s with pH is too small to be explained by Eq. 5. In view of the precision of determination of k_s value no conclusive statement can be given at present.

In a.c. voltammetry a slight difference in height between the waves of negative-going and positive-going voltage scan were observed (Fig. 9). This can be explained by assuming that there are two conformations I and II of adsorbed apoferredoxins each for oxidized form, Apo-Fd(SHg)$_{n_c}$, and reduced form, Apo-Fd(SH)$_{n_c}$,

$$\begin{array}{ccc} (\text{Apo-Fd(SHg)}_{n_c})_\mathrm{I} & \overset{n_c}{\rightleftharpoons} & (\text{Apo-Fd(SH)}_{n_c})_\mathrm{I} \\ \downarrow\uparrow & & \downarrow\uparrow \\ (\text{Apo-Fd(SHg)}_{n_c})_\mathrm{II} & \overset{n_c}{\rightleftharpoons} & (\text{Apo-Fd(SH)}_{n_c})_\mathrm{II}. \end{array}$$

The waves of negative-going and positive-going scan can be assigned to

$$(\text{Apo-Fd(SHg)}_{n_c})_\mathrm{I} \overset{n_c}{\rightleftharpoons} (\text{Apo-Fd(SH)}_{n_c})_\mathrm{I} \rightleftharpoons (\text{Apo-Fd(SH)}_{n_c})_\mathrm{II}$$

and

$$(\text{Apo-Fd(SH)}_{n_c})_\mathrm{II} \overset{n_c}{\rightleftharpoons} (\text{Apo-Fd(SHg)}_{n_c})_\mathrm{II} \rightleftharpoons (\text{Apo-Fd(SHg)}_{n_c})_\mathrm{I},$$

respectively. The difference between the two peak heights should be due to the difference between the apparant standard rate constants of the two processes.

We are grateful to Associate Professor Yoshiki Tani and Dr. Sakae Shimizu for help in growing the Clostridium pasteurianum and to Dr. Masaaki Takahashi for help in the purification of spinach ferredoxin. This work was supported by a Grant-in-Aid from the Ministry of Education.

References

1) For reviews *cf.* "Iron-Sulfur Proteins," ed by W. Lovenberg, Academic Press, New York and London, Vols. I and II(1973) and III(1977).

2) N. A. Stombaugh, J. E. Sundquist, R. H. Burris, and W. H. Orme-Johnson, *Biochemistry*, **15**, 2633 (1976) and references therein.

3) P. D. Weitzman, I. R. Kenedy, and R. A. Caldwell, *FEBS Lett.*, **17**, 241 (1971).

4) H. Dalton and J. Zubieta, *Biochim. Biophys. Acta*, **322**, 133 (1973).

5) Y. W. Chien, *J. Pharm. Sci.*, **65**, 1471 (1976).

6) B. A. Kiselev, *Biofizika*, **21**, 35 (1976).

7) C. L. Hill, J. Renaud, R. H. Holm, and L. E. Mortenson, *J. Am. Chem. Soc.*, **99**, 2549 (1977).

8) P. Bianco and J. Haladjian, *Biochem. Biophys. Res. Commun.*, **78**, 323 (1977).

9) a) W. L. Underkofler and I. Shain, *Anal. Chem.*, **37**,

218 (1965); b) A. M. Bond, R. J. O'Halloran, I. Ruzic, and D. E. Smith, *Anal. Chem.*, **48**, 872 (1976).
10) S. G. Mayhew, *Anal. Biochem.*, **42**, 191 (1971).
11) B. B. Buchanan and D. I. Arnon, *Methods Enzymol.*, **23**, 413 (1971).
12) J. Koryta, *Collect. Czech. Chem. Commun.*, **18**, 206 (1953).
13) B. A. Kuznetsov, *Experientia, Suppl.*, **18**, 381 (1971).
14) M. Senda, T. Ikeda, and H. Kinoshita, *Bioelectrochem. Bioenerg.*, **3**, 253 (1976).
15) a) E. Laviron, *J. Electroanal. Chem. Interfacial Electrochem.*, **52**, 355 (1974); b) S. Srinivasan and E. Gileadi, *Electrochim. Acta*, **11**, 321 (1966).
16) B. A. Kuznetsov, N. M. Mestechkina, and G. P. Shumakovich, *Bioelectrochem. Bioenerg.*, **4**, 1 (1977).
17) W. Lovenberg, B. B. Buchanan, and J. C. Rabinowitz, *J. Biol. Chem.*, **238**, 3899 (1963).
18) Ref. 1, Vol. II, p. 37.
19) F. Sheller, H-J. Prumke, H. E. Schmidt, and P. Mohr, *Bioelectrochem. Bioenerg.*, **3**, 328 (1976).
20) A. P. Brown and F. C. Anson, *Anal. Chem.*, **49**, 1958 (1977).
21) M. Senda and P. Delahay, *J. Phys. Chem.*, **65**, 1580 (1961).